Poly(ethylene-*co*-tetrafluoroethylene)-Derived Radiation-Grafted Anion-Exchange Membrane with Properties Specifically Tailored for Application in Metal-Cation-Free Alkaline Polymer Electrolyte Fuel Cells

John R. Varcoe,*,† Robert C. T. Slade,† Eric Lam How Yee,† Simon D. Poynton,† Daniel J. Driscoll,† and David C. Apperley‡

Department of Chemistry, The University of Surrey, Guildford, Surrey GU2 7XH, United Kingdom, and Solid State NMR Service, Department of Chemistry, University of Durham, Durham DH1 3LE, United Kingdom

Received October 8, 2006. Revised Manuscript Received January 18, 2007

A new class of stable poly(ethylene-*co*-tetrafluoroethylene)-based alkaline anion-exchange membrane (AAEM) with enhanced tensile strength has been synthesized in response to the poor mechanical properties of previously reported poly(tetrafluoroethylene-*co*-hexafluoropropylene) radiation-grafted AAEMs; this type of AAEM exhibits significant through-plane conductivities (up to 0.034 ± 0.004 S cm^{-1} at 50 °C in water: conductivities that match requirements for application in fuel cells). The methanol permeabilities of this new AAEM class were found to be substantially reduced relative to Nafion-115 proton-exchange membranes; this offers the prospect that thin, low-resistance membranes may be used in direct methanol alkaline fuel cells with reduced methanol crossover. The fuel cell power performances obtained in a H_2/O_2 single fuel cell at 50 °C with this AAEM is now within 1 order of magnitude of state-of-the-art Nafion-based fuel cells. It is evident that the alkaline ionomers are not the primary performance limiters of alkaline membrane fuel cells; performances are currently limited by the electrode architectures that have been optimized for use in PEM fuel cells but not alkaline fuel cells. The need for electrodes and catalyst structures that have been specifically tailored for use in AAEM-containing fuel cells is highlighted.

Introduction

There is substantial interest in the application of alkaline membranes (membranes that conduct hydroxide ions, the high pH equivalent to proton-exchange membranes such as Nafion by DuPont) in fuel cells. The advantages and disadvantages of this application of alkaline membranes have been explained in detail in a previous review[1] and so the main points only are summarized: (1) Potentially reduced methanol permeability (relevant to application in direct methanol fuel cells, DMFCs). (2) A significant change in water management (water generated at the anode and consumed at the cathode). (3) Improved electrokinetics leading to the use of the following:

(a) Non-Pt metal catalysts in fuel cells (proven—a recent article by the authors have demonstrated that Ag/C cathode catalysts perform comparatively to Pt/C with alkaline membranes);[2] this potentially extends the opportunity for selective catalysts that would facilitate the development of mixed-reactant fuel cells.[3]

(b) Higher energy density fuels compared to methanol, including potentially carbon-neutral bioethanol,[4] in direct alcohol fuel cells. Preliminary studies in our laboratories indicate that the power density outputs of alkaline membrane fuel cells at 50 °C are higher with ethanol than with methanol, a situation that is the reverse of that found with Nafion-based fuel cells.

Alkaline anion-exchange membranes (AAEM) based on the widely utilized radiation-grafting methodology[5] involve the modification of preformed films (no film formation step required) and contain no M^{n+} counterions, such as K^+ or Na^+ (as found in AAEMs based on KOH-doped polybenzimidazole[6]), which would cause the same carbonate precipitation problems as found with traditional aqueous KOH-electrolyte alkaline fuel cells when operated with CO_2-containing air or with methanol electro-oxidation to CO_2 at the anode.[7]

Previous membrane investigations in our laboratory have concluded that AAEMs produced from the radiation grafting of vinylbenzyl chloride, VBC, onto partially fluorinated poly(vinylidene fluoride), PVDF, preformed films with subsequent quaternization with trimethylamine were unsatisfactory

* To whom correspondence should be addressed. Tel: +44 1483 682616. Fax: +44 1483 686851. E-mail: j.varcoe@surrey.ac.uk.
† The University of Surrey.
‡ University of Durham.

(1) Varcoe, J. R.; Slade, R. C. T. *Fuel Cells* **2005**, *5*, 187.
(2) Varcoe, J. R.; Slade, R. C. T.; Wright, G. W.; Chen, Y. *J. Phys. Chem. B* **2006**, *110*, 21041.
(3) Shukla, A. K.; Raman, R. K.; Scott, K. *Fuel Cells* **2005**, *4*, 436.
(4) Pearce, F. *New Sci.* **2006**, no. 2570, 36.
(5) Dargaville, T. R.; George, G. A.; Hill, D. J. T.; Whittaker, A. K. *Prog. Polym. Sci.* **2003**, *28*, 1355.
(6) Xing, B.; Savadogo, O. *Electrochem. Commun.* **2000**, *2*, 697.
(7) Gülzow, E.; Schultz, M. *J. Power Sources* **2004**, *127*, 243.

10.1021/cm062407u CCC: $37.00
Published on Web 04/24/2007

Scheme 1. Synthesis of ETFE-Based Radiation-Grafted Alkaline Anion-Exchange Membrane (ETFE−AAEM)

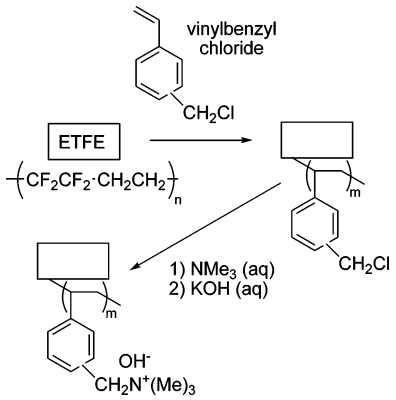

as the AAEMs produced were physically weak due to chemical degradation (serious dehydrofluorination side reactions in the presence of alkali).[8] This led to development of the fully fluorinated poly(tetrafluoroethylene-*co*-hexafluoropropylene), FEP, analogues of the above AAEMs; these exhibited superior chemical and thermal stabilities[9] and promising conductivities (up to 23 mS cm^{-1} at 50 °C in water—fully hydrated AAEMs).[10] Unfortunately, due to the low radiation resistance of FEP, the resulting AAEMs were still brittle and often contained small tears; this effectively prevented fuel cell testing of these membranes on safety grounds (even after extensive optimization studies). The source of this radiation intolerance is that undesirable C−C backbone bond breakage occurs in preference to the C−F bonds when fully fluorinated polymers are subjected to radiation. Despite our earlier studies suggesting partially fluorinated precursor films were not well-suited to the production of radiation-grafted AAEMs, poly(ethylene-*co*-tetrafluoroethylene), ETFE, films exhibit superior radiation resistance (C−H bonds are present that break, when irradiated in air to form the peroxy radicals, in preference to the C−C bonds) and have been successfully used to produce radiation-grafted proton-exchange membranes with enhanced physical stability over FEP analogues.[11] Even though ETFE can be considered to be a "head-to-head, tail-to-tail" isomeric form of PVDF, it is well-known that the properties of these two polymers are very different.[12]

This article extends preliminary work[13] and describes in detail the successful synthesis of a physically stable AAEM, based on the radiation grafting of VBC onto ETFE films with subsequent quaternization with trimethylamine (Scheme 1) that exhibits significant conductivity with no loss of thermal and chemical stability. This constitutes a breakthrough that allows the successful application of this form of AAEM in fuel cells. The alkaline membrane produced was chemically characterized using solid-state NMR and Raman spectroscopies. Ex situ physical characterizations included thermal and stress−strain analyses and measurement of the ionic conductivity in water, ion-exchange capacity, and methanol permeability. Preliminary fuel cell test data (H_2/O_2 and DMFC) with this AAEM are also presented.

Materials and Methods

The synthetic protocol for the AAEMs has been described in detail previously[9] and will only be summarized here along with details of a few recent optimizations. Reverse osmosis (RO) water was used throughout this study. The ETFE film (50 μm thick Nowoflon ET-film 6235, Nowofol Kunststoffprodukte GmbH, Germany) was irradiated with a ^{60}Co γ-ray source (Defence Academy of the United Kingdom, Cranfield University, Shrivenham, Swindon, UK) at a temperature of 23 ± 1 °C to a total dose of 7 Mrad (70 kGy) at a dose rate of 0.04 Mrad h^{-1} (0.4 kGy h^{-1}) and was stored at −38 ± 2 °C until required (after transportation in solid CO_2); storage under these conditions is adequate for retention of the radicals for at least 12 months.[14] Vinylbenzyl chloride (VBC, Dow Chemicals, Lot # SA12012U01: 96.7%, meta/para ratio = 1, stabilized with 75 ppm 4-*tert*-butylcatechol and 811 ppm nitromethane, 132 ppm residual water content) was stored in a refrigerator and used undiluted as the grafting monomer. Grafting was conducted by immersion of the irradiated ETFE into the VBC, purging with nitrogen for 2 h, and then heating the sealed grafting vessel at 60 °C for 67 h. Note: while grafting at 50 °C was the optimum temperature with FEP and VBC,[9] this was found not to be the case with ETFE and VBC; very little grafting was observed at 50 °C and small scale tests indicated that 60 °C was optimal, as has been previously reported with styrene-grafted ETFE.[14] The intermediate ETFE-*g*-poly(VBC) membrane was produced as a white translucent membrane with a degree of grafting, d.o.g. = $100\% \times (\text{mass}_{\text{grafted}} - \text{mass}_{\text{initial}})/\text{mass}_{\text{initial}})$, of 23.6%. No further optimization was conducted at this stage as 23.6% represents a good level of grafting; our experience, and that of others,[15] indicates that grafting levels below 20% lead to reduced conductivities, while grafting levels above 30% lead to excessive swelling in water and brittle ion-exchange membranes.

The ETFE-*g*-poly(VBC) intermediate membrane was subsequently submerged in aqueous trimethylamine (Acros Organics, 50 wt %) for 4 h; this is less than the 24 h previously reported as recent further optimization studies have confirmed that 4 h is adequate for maximum quaternization levels (minimization of such treatment times is always desirable). After the membrane was washed several times in water, the resulting hydrophilic anion-exchange membrane (now as chloride-form and obtained as orange transparent membranes) was boiled in water for 1 h (to remove residual trimethylamine and to fully hydrate the membrane) and was finally washed in water several more times. Conversion to the alkaline form, within 1 day of required use, was conducted as follows: the chloride-ion form anion-exchange membrane was submerged in aqueous potassium hydroxide (Fisher Scientific, 1.0 mol dm^{-3}, at least 10 times excess) for 1 h with two changes of KOH(aq) during this period to ensure complete ion exchange. The resulting AAEM was then soaked in water for 1 h with at least two changes of water to remove any lingering potassium hydroxide. The final AAEM "as-synthesized" was obtained as dark brown/orange membrane and was stored in the dark in water until required; the AAEM was not allowed to dry out at any point before measurements were conducted unless otherwise stated.

(8) Danks, T. N.; Slade, R. C. T.; Varcoe, J. R. *J. Mater. Chem.* **2003**, *13*, 712.
(9) Herman, H.; Slade, R. C. T.; Varcoe, J. R. *J. Membr. Sci.* **2003**, *218*, 147.
(10) Slade, R. C. T.; Varcoe, J. R. *Solid State Ionics*. **2005**, *176*, 585.
(11) Chen, J.; Asano, M.; Maekawa, Y.; Yoshida, M. *J. Membr. Sci.* **2006**, *269*, 194.
(12) Brandrup, J.; Immergut, E. H. *Polymer Handbook 3rd Edition*; John Wiley and Sons: New York, 1989; p V48.
(13) Varcoe, J. R.; Slade, R. C. T. *Electrochem. Commun.* **2006**, *8*, 839.
(14) Horsfall, J. A.; Lovell, K. V. *Eur. Polym. J.* **2002**, *38*, 1671.
(15) Gubler, L.; Prost, N.; Gürsel, S. A.; Scherer, G. G. *Solid State Ionics* **2005**, *176*, 2849.

Routine Raman spectra were recorded on a Perkin-Elmer System 2000 FT-Raman/near-IR spectrometer with a laser power of 1200 mW and a resolution of 4 cm^{-1}. Liquid and membrane samples were mounted in the beam in glass vials at ambient temperature and pressure (the Raman spectrum of the dark brown AAEM was recorded with the membrane immersed in water to prevent the laser burning the sample). High-resolution solid state $^{13}C\{^1H\}$ and $^{15}N\{^1H\}$ nuclear magnetic resonance (NMR) data were collected at the EPSRC solid-state service at the University of Durham on a Varian *Innova* spectrometer (with a ^1H resonant frequency of 300 MHz). $^{19}F\{^1H\}$ spectra were recorded on a Varian *Infinity plus* (with a ^1H resonant frequency of 500 MHz). $^{19}F\{^1H\}$ spectra ($CFCl_3$ shift reference) were recorded using direct polarization and a magic angle spinning rate of 14 kHz. $^{13}C\{^1H\}$ (TMS as a shift reference) and $^{15}N\{^1H\}$ (CH_3NO_2 as a shift reference) spectra were recorded using cross-polarization (with a flip-back pulse after acquisition) and a spinning rate of 5 kHz. Measurements were carried out at ambient temperature and pressure. To record spectra of the anion-exchange membranes, the samples were dried in the open atmosphere, to remove excess water, before measurement.

The ion-exchange capacity, defined in this study as mol(OH^-) g^{-1}(dry HAAEM), was determined using the standard back-titration technique reported previously.[10] Water uptake, $WU = 100\% \times (mass_{wet} - mass_{dry})/mass_{dry}$), was determined gravimetrically from the mass difference between samples of the hydrated AAEM "as-synthesized" and when dried at a relative humidity (RH) of 0% (i.e. stored over anhydrous $CaCl_2$ in a desiccator) for 7 days. The thicknesses of the wet and dry AAEM were measured using an outside micrometer. Thermogravimetric analysis was conducted on a TA Instruments TGA Q500, on 10−20 mg samples placed in Pt crucibles; the measurements were conducted at 2 °C min^{-1} in flowing air (60 mL min^{-1}). A TA-XTplus Texture Analyzer (Stable Micro Systems Ltd., Godalming, UK) was employed to analyze the tensile stress−strain behavior of dumbbell-shaped specimens of the hydrated ionomers at room temperature; a constant crosshead speed of 1 mm s^{-1} was used for all samples. Due to the limited amount of sample available, the tests were conducted on non-standard-sized samples (width = 3.2 mm and length = 15 mm); as this does not comply with ASTM D 882, the results cannot be compared with values reported in the literature. However, all ionomer samples were tested in an identical fashion and so the properties of the ionomers can be compared relative to one another. The conductivity of the fully hydrated AAEM was determined via impedance spectroscopy (Solartron 1260 frequency response analyzer allied with a Solartron 1287 potentiostat/galvanostat for control of the d.c. bias) using the same procedure as reported previously in a detailed study of the conductivities of FEP-based AAEMs.[10] The permeation cell set up and methodology for determining methanol permeabilities of membranes was as described in detail by Nasef et al.;[16] a CSi 200 Series gas chromatograph with flame ionization detector and a SolGel-WAX capilliary column (SGE, Ringwood, Australia, 30 m × 0.25 mm i.d. and 1 μm film thickness) was used for determination of methanol concentrations in aqueous solutions. Any errors given in the text and tables relate to the sample standard deviation for at least three replicate measurements on the membrane.

Directly before fuel cell testing the AAEMs were converted to the OH^- form, from the stored Cl^- form, as described above. The electrodes (25 cm^2, E-Tek 4 mg cm^{-2} unsupported PtRu-alloy-coated carbon cloth anode electrodes, E-Tek 4 mg cm^{-2} unsupported Pt-black-coated carbon cloth cathode electrodes—both containing a proprietary loading of PTFE used as a binding material) were coated with a water-insoluble alkaline interface polymer as previously reported:[17] Each electrode was coated with 0.8 ± 0.1 mg cm^{-2} poly(vinylbenzyl chloride) (Aldrich, U.K.) using a spray gun and ethyl acetate as solvent. To form the cross-linked (water insoluble) alkaline interface polymer, the treated electrodes were then immersed in *N*,*N*,*N*′,*N*′-tetramethylhexane-1,6-diamine (Acros Organics, U.K., caution: toxic) for 12 h at room temperature, washed with water, and ion-exchanged to the OH^- form using the procedure described for the AAEM above. Cross-linked anion-exchange materials produced using this particular diamine are reported to have enhanced thermal stability when in alkali compared to other diamines such as *N*,*N*,*N*′,*N*′-tetramethylethane-1,2-diamine.[18] The AAEM and treated electrodes were assembled into the fuel cell fixture at a torque of 5.5 N m without pre-pressing into MEAs; this is unusual, but the electrodes and this particular AAEM did not laminate unless pressed at 100 °C where they become black in color. Preliminary experiments with another AAEM[17] have shown that the performance is similar between fuel cells tested with pre-pressed and unpressed MEAs, so the latter case was selected for this study to avoid damage to the AAEM. As the MEAs were assembled in the fuel cell fully swollen and the MEAs are tested under conditions RH = 100%, the membranes are fully swollen during the entire test period. Therefore, the contact between the electrodes and membrane does not vary during the tests.

Fuel cell testing was conducted with an Arbin Instruments (College Station, TX) Fuel Cell Test Station (FCTS). The MEAs were mounted in a 5 × 5 cm test fixture containing graphite blocks with machined triple serpentine flow channels (1 mm channel width, 1 mm channel height, 1.5 mm rib width) and gold-coated current collector plates. The test fixture was assembled with retaining bolts tightened to a torque of 5.5 N m. Fuel cell testing was conducted at a fuel cell temperature of 50 °C with H_2 and O_2 gases (laboratory grade, BOC) supplied at 2 dm^3 min^{-1} flow rates and RH = 100% (dew point temperature = 50 ± 1 °C); the gas lines between the dew point humidifiers and the fuel cell fixture were heated to 10 °C above the set dew point to minimize condensation in the supply pipes. These gas flows correspond to high gas and cathode water stoichiometries ($\lambda_{O_2,cathode} = 23$, $\lambda_{H_2,anode} = 11.5$, and $\lambda_{H_2O,cathode} = 1.6$ at a current density, *i*, of 1 A cm^{-2}, the water stoichiometry calculated from the gas dew points and assuming no back transport of water from the anode to the cathode). For direct methanol fuel cell tests the anode was supplied with aqueous methanol (2 mol dm^{-3}, 10 cm^3 min^{-1}, $\lambda_{MeOH,anode} = 7.8$ at $i = 1$ A cm^{-2}) that was preheated to 50 ± 1 °C. These high stoichiometries were deliberately chosen to minimize mass-transport interferences, which is valid for an initial membrane development study. The fuel cell temperature of 50 °C was selected to ensure minimal thermal degradation of the membranes during testing; current alkali anion-exchange materials containing β-hydrogen-atoms (as in the interface alkaline polymer used in this study, the β-hydrogens allow Hofmann elimination reactions to occur)[1] exhibit acceptable thermal stability only when kept below 60 °C (as found for numerous anion-exchange membranes and resins).[19,20] Beginning-of-life cell voltage (V_{cell}, V) and power density (P_{cell}, mW cm^{-2}) vs current density (*i*, mA cm^{-2}) steady-state polarization curves were collected under

(16) Nasef, M. M.; Zubir, N. A.; Ismail, A. F.; Khayet, M.; Dahlan, K. Z. M.; Saidi, H.; Rohani, R.; Ngah, T. I. S.; Sulaiman, N. A. *J. Membr. Sci.* **2006**, *268*, 96.

(17) Varcoe, J. R.; Slade, R. C. T.; Lam How Yee, E. *Chem. Commun.* **2006**, 1428.

(18) Komkova, E. N.; Stamatialis, D. F.; Strathmann, H.; Wessling, M. *J. Membr. Sci.* **2004**, *244*, 25.

(19) Tomoi, M.; Yamaguchi, K.; Ando, R.; Kantake, Y.; Aosaki, Y.; Kubota, H. *J. Appl. Polym. Sci.* **1997**, *64*, 1161.

(20) Zagorodni, A. A.; Kotova, D. L.; Selemenev, V. F. *React. Funct. Polym.* **2002**, *53*, 157.

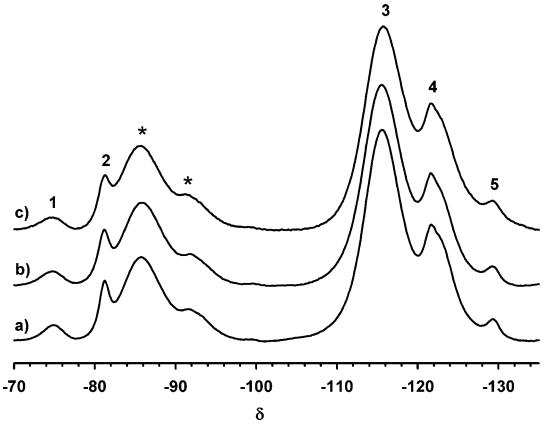

Figure 1. $^{19}F\{^1H\}$ direct-polarization MAS solid-state NMR spectra of (a) ETFE, (b) ETFE-*g*-poly(VBC), and (c) ETFE-*g*-poly(vinylbenzyltrimethylammonium chloride) anion-exchange membrane. * denotes spinning side bands.

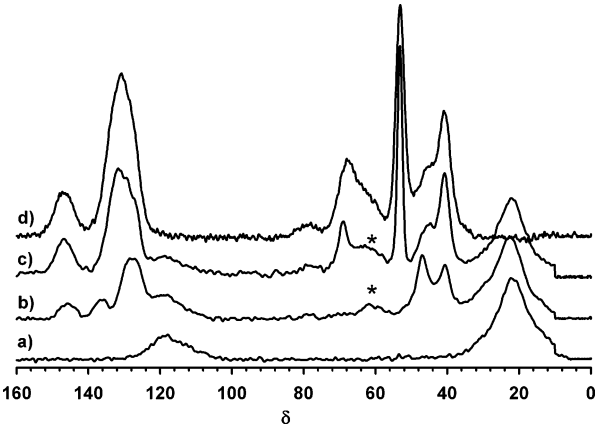

Figure 2. $^{13}C\{^1H\}$ cross-polarization MAS solid-state NMR spectra of (a) ETFE, (b) ETFE-*g*-poly(VBC), (c) ETFE-*g*-poly(vinylbenzyltrimethylammonium chloride) anion-exchange membrane, and (d) commercially available poly(benzyltrimethylammonium chloride). * denotes spinning side bands.

galvanostatic control (constant reaction rates) using the FCTS's integral electronic load with data points being recorded after V_{cell} equilibrated to a constant potential (normally 5−10 min); before the i/V_{cell} curves were recorded, each MEA was "conditioned" by operating at high i (potentiostatic cell discharge at $V_{cell} = 50$ mV) until the current density had stabilized at a constant value (1−2 h was required for the AAEM−MEA); this conditioning step allows all the ionic materials in the electrodes to fully hydrate in a dynamic environment where ions (and associated water molecules) are moving. All current densities are referred to the geometric area of the electrodes (25 cm^2).

Results and Discussion

The tear-free AAEM produced from the ETFE-*g*-poly(VBC) intermediate with degree of grafting of 23.6% yielded an ion-exchange capacity (IEC) of $(1.03 \pm 0.11) \times 10^{-3}$ mol_{OH-} g^{-1} (cf. 0.92 mol_{H+} g^{-1} for Nafion-115[21]). The water uptake (WU) of the AAEM was 40 ± 4% (which corresponds to a water content of $\lambda = 22 \pm 3$ water molecules per OH^- ion)[10], which is lower than that found with a FEP−AAEM of a similar grafting level (degree of grafting = 23.9%, IEC = $(1.02 \pm 0.03) \times 10^{-3}$ mol_{OH} g^{-1}, WU = 56 ± 5%, $\lambda = 30 \pm 4$); this was expected due to the higher crystallinity of ETFE compared with that of FEP and this lowered swelling in water is expected to further translate into higher strength. The thickness of the wet membrane "as-synthesized" was 78 ± 3 μm, which reduced to 63 ± 3 μm on dehydration (again cf. the FEP analogue of similar grafting level: 86 ± 2 μm wet, 65 ± 2 μm dry); this again is indicative of the reduced swelling (desirable) of the ETFE−AAEMs compared to the FEP−AAEMs. The thickness was fully recovered on rehydration via immersion in water at room temperature.

Chemical degradation of the PVDF backbone in the production of chemically unstable PVDF−AAEMs was proven using solid-state NMR.[8] This technique was therefore applied to the ETFE−AAEM. The $^{19}F\{^1H\}$ direct polarization NMR spectra of the ETFE, ETFE-*g*-poly(VBC), and the resulting anion-exchange membrane are presented in Figure 1. The same bands with the same line widths were observed in all three spectra; this indicates that the ETFE backbone is not undergoing significant changes on grafting and amination, as was found with the FEP analogues but not the PVDF analogues.[8] This confirms the different behavior of ETFE compared with that of PVDF when used to form radiation-grafted AAEMs. The bands (labeled 3, 4, and 5 in Figure 1) at $\delta_F = -116$, -122, and -130 relate to CF_2 in the various environments.[22] The two small bands (labeled 1 and 2 in Figure 1) at $\delta_F = -75$ and -81 relate to CF_3 atoms.[23] These bands belong to additional components of the commercial ETFE membrane; the identity of these components is proprietary. It is important to note that the results reported in this paper are only strictly valid when this particular type of commercial ETFE is used to form AAEMs. Spinning side bands were identified by observing band shifts in spectra when recorded with varying MAS probe spinning rates.

The $^{13}C\{^1H\}$ CP-MAS NMR spectra of the ETFE, ETFE-*g*-poly(VBC), the resulting anion-exchange membrane, and commercially available poly(vinylbenzytrimethylammonium chloride) (Scientific Polymer Products Inc.) are presented in Figure 2. As the spectrometer available possessed only one decoupling channel and $\{^{19}F\}$-decoupling was not present, the $C-F$ carbon band observed at $\delta_C = 118$ was relatively broad; the large band at $\delta_C = 22$ in the $^{13}C\{^1H\}$ spectrum of ETFE relates to the $C-H$ carbons; the bands match those previously reported in the literature.[24] For the ETFE-*g*-poly(VBC), the extra bands observed at $\delta_C = 146$, 135, 128, 47, and 41 relate to the poly(VBC) component and match the bands previously found in the $^{13}C\{^1H\}$ CP-MAS NMR spectrum of the FEP analogue.[8] The $^{13}C\{^1H\}$ CP-MAS NMR spectrum of the anion-exchange membrane exhibits the bands found in the $^{13}C\{^1H\}$ CP-MAS NMR spectrum of poly(vinylbenzytrimethylammonium chloride), at $\delta_C = 147$, 130, 68, 53, 45, and 41, superimposed on the ETFE bands, confirming that grafting and quaternization produced the expected functionality; the low line width band

(21) Silva, R. F.; De Francesco, M.; Pozio, A. *J. Power Sources* **2004**, *134*, 18.
(22) Aimi, K.; Ando, S. *Magn. Reson. Chem.* **2004**, *42*, 577.
(23) Isemura, T.; Jitsugiri, Y.; Yonemori, S. *J. Anal. Appl. Pyrolysis* **1995**, *33*, 103.
(24) Feng, J.; Chan, C. M. *Polymer* **1997**, *38*, 6371.

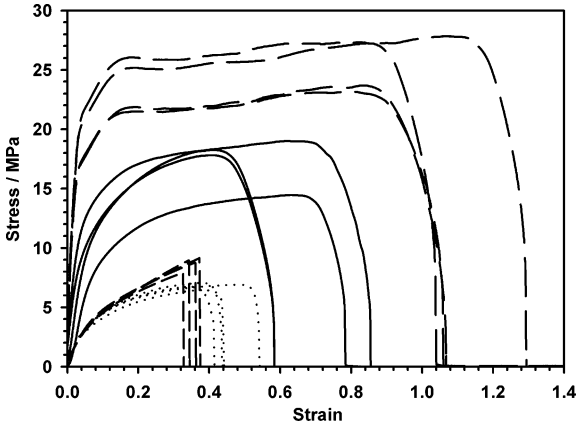

Figure 3. Stress−strain curves for the precursor ETFE (long-dashed lines − − −), the fully hydrated samples of ETFE−AAEM (solid lines), Nafion-115 (short-dashed lines - - -), and an FEP−AAEM (dotted lines ···).

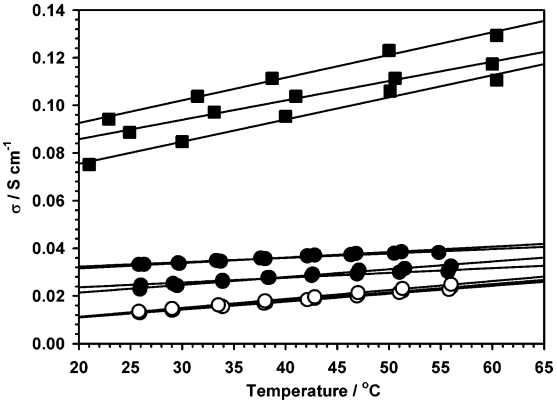

Figure 4. Conductivities in water (fully hydrated), at increasing temperatures and determined using electrochemical impedance spectroscopy, of the ETFE−AAEM OH^- form (●, four replicate measurements), the ETFE−AAEM in CO_3^{2-} form (○, three replicate measurements), and Nafion-115 in H^+ form (■, three replicate measurements). Lines are guides to the eye only.

at $\delta_C = 53$ is highly characteristic of N(CH_3) carbons, and this was further confirmed on undertaking another dipolar diphasing experiment. A final delayed contact experiment was conducted to look for any variations in the $T_{1\rho}$ of the ^1H atoms that would indicate sample inhomogeneity; all the components behaved with a common $T_{1\rho}$, confirming the homogeneous sample expected for the synthetic methodology used. The $^{15}N\{^1H\}$ spectrum (not shown) of the anion-exchange membrane exhibited the expected single band at $\delta_N = -328$, exactly as observed for the FEP analogue.[8]

The membranes were also investigated using Raman spectroscopy. As expected, the spectrum of the ETFE-*g*-poly(VBC) was comprised of the superimposed spectra of commercial poly(vinyl benzyl chloride) (Aldrich) and ETFE, while the spectrum of the AAEM was comprised of the superimposed spectra of ETFE and commercial poly(vinylbenzyltrimethylammonium chloride). Of particular significance was that the CH_2Cl deformation band at 1268 cm^{-1} in the spectrum of ETFE-g-poly(VBC) disappeared on amination, confirming complete reaction of the CH_2Cl groups.[8,9] These Raman results further confirmed successful grafting and amination.

Thermogravimetry (2 °C min^{-1} in flowing air) was used to probe the *short-term* thermal stability of the membranes. The TG trace of ETFE showed that polymer degradation commenced at 280 ± 10 °C, which matches previously reported degradation data.[25] Degradation commenced at 195 ± 10 °C for the intermediate membranes produced when ETFE was grafted with VBC; this is consistent with FEP-*g*-poly(VBC) membranes with degrees of grafting of 20−30%.[9] Finally, the degradation of the AAEM commences at 130 ± 10 °C, which is again consistent with FEP-based AAEMs reported previously[9] and is above the 60 °C maximum operating temperatures envisioned for these membranes.

Tensile stress−strain curves were obtained to give an indication of the relative strengths of the AAEM, Nafion, ETFE precursor film, and a FEP-based AAEM (Figure 3, all ionomers fully hydrated). It is immediately evident that the ETFE−AAEM can withstand higher tensile stresses than both the FEP-based AAEM and Nafion-115. The move from the use of precursor FEP to the use of ETFE has led to fundamentally stronger membranes; this is fully consistent with other studies that have investigated sulfonic acid radiation-grafted PEMs produced using different types of precursor films.[26] As anticipated, the ETFE−AAEM can withstand lower tensile stresses than the ETFE precursor membrane, showing that the process of radiation grafting and quaternization affects the mechanical properties of the membrane. The ionomers were fully hydrated before testing. However, due to the small size of the samples, the ionomers would experience some dehydration during mounting and testing; this accounts for the variations in the responses of samples of the same ionomer (as confirmed by subsequent tests on other ionomer membranes). It is well-known that the properties of such ionomers are very sensitive to humidity.[21] The results discussed so far clearly indicate that ETFE can be successfully radiation-grafted with vinylbenzyl choride to form alkaline anion-exchange membranes in the same manner as FEP, but with a reduction in undesirable swelling in water, enhanced tensile strength, no chemical degradation of the base polymer backbone, and no decrease in short-term thermal stability.

Membrane ionic conductivity, σ/S cm^{-1}, is defined by

$$\sigma = \frac{t}{R \times A} \tag{1}$$

where t/cm is the fully hydrated membrane thickness, R/Ω is the membrane resistance through the thickness of the membrane (through plane not surface resistance), as determined by impedance spectroscopy, and A/cm^2 is the area. A full comparison between Nafion-115 and the AAEM of the conductivities below 60 °C is displayed in Figure 4. Selected values are presented in Table 1. As expected, the AAEM was lower in conductivity than Nafion-115, in-line with the FEP-based AAEMs evaluated previously.[10] A widely perceived problem with the application of AAEMs in direct methanol fuel cells is that the electro-oxidation of methanol

(25) *Fluoroplastics Vol 2 − Melt Processible Fluoropolymers*; Ebnesajjad, S., Eds.; William Andrew Publishing: Norwich, NY, 2003; pp 408.

(26) Chen, J.; Asano, M.; Maekawa, Y.; Yoshida, M. *J. Membr. Sci.* **2006**, *277*, 249.

Table 1. A Comparison of Selected Fuel-cell-relevant Physical Parameters

	AAEM (OH^-)	AAEM (CO_3^{2-})	Nafion-115
σ_{20}[a]/S cm^{-1}	0.027 ± 0.005	0.0117 ± 0.0002	0.076 ± 0.009
σ_{50}[a]/S cm^{-1}	0.034 ± 0.004	0.0217 ± 0.0008	0.111 ± 0.009
10^7 P_{20}[b]/cm^2 s^{-1}	5.4 ± 2.8		19 ± 9
10^{-4} Φ_{20}[c]/S cm^{-3} s	5.0 ± 2.8		4.0 ± 2.0
WU[d] (%)	40 ± 4		36 ± 4
MU[e] (%)	31 ± 4		71 ± 2

[a] Conductivities of the ionomers in water (fully hydrated). [b] Methanol permeability. [c] The DMFC performance parameter defined in eq 3. [d] Gravimetric water uptakes of the fully hydrated membranes. [e] Gravimetric methanol uptakes of the fully swollen membranes. Subscripts denote measurement temperatures in °C.

in the anode, producing CO_2 as a product, would cause carbonation of the AAEM and this would lead to severely decreased conductivities. Therefore, the conductivities of the AAEM were investigated in the CO_3^{2-} anion form (ion-exchanged with potassium carbonate (1 mol dm^{-3}) rather than potassium hydroxide). Preliminary results (Figure 4) indicated that the conductivities are not significantly decreased in the CO_3^{2-} form compared to the OH^- form; therefore, an in depth investigation into the properties of AAEMs in CO_3^{2-} form has been instigated and data will be reported in due course.

Empirical activation energies can be calculated as previously reported,[10]

$$E_a = -b \times R \tag{2}$$

where R is the molar gas constant 8.3145 J K^{-1} mol^{-1} and b is the slope of $\ln(\sigma/\text{S cm}^{-1})$ vs $(1000/T)/\text{K}^{-1}$ plots determined using standard linear regression techniques; values of 7.1 ± 1.4 and 6.2 ± 2.4 kJ mol^{-1} were obtained for Nafion-115 and the AAEM(OH^-) respectively. The value for the AAEM was the same as that of Nafion-115 (within experimental error) and was lower than the values previously reported for FEP-based AAEMs (12.6 ± 0.6 kJ mol^{-1}).[10] A higher empirical activation energy of 16.1 ± 0.4 kJ mol^{-1} was determined for the carbonate-form AAEM.

The ex situ methanol permeabilities at 20 °C of the AAEM and Nafion-115 are presented in Table 1 along with the corresponding "DMFC performance parameter" Φ which is defined as[16]

$$\Phi = \frac{\sigma}{P} \tag{3}$$

where P/cm^2 s^{-1} is the methanol permeability; the higher the value of Φ, the higher the DMFC performance will be with defined catalysts and when the membrane properties constitute the principle factors that dictate fuel cell performance. The (thickness-independent) methanol permeability is the product $P = DK$ where D is the methanol diffusivity and K the partition coefficient.[27]

It is evident that methanol transport through the AAEM is reduced significantly compared to Nafion; hence, thinner membranes can feasibly be used in DMFCs, offsetting the lower conductivities. Within experimental errors in the values of Φ, there is little difference between the two membranes.

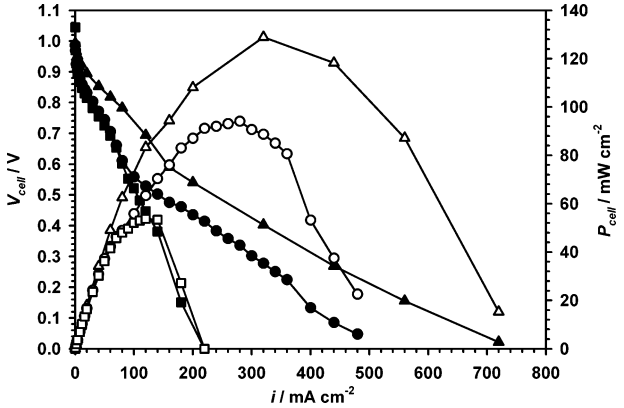

Figure 5. Fuel cell performances (ambient pressures and 50 °C; anode: 4 mg cm^{-2} unsupported PtRu, H_2 supplied at 2 dm^3 min^{-1}, and RH = 100%; cathode: 4 mg cm^{-2} unsupported Pt black, O_2 supplied at 2 dm^3 min^{-1}, and RH = 100%) with the following: (●) the ETFE−AAEM (78 ± 3 μm fully hydrated thickness) synthesized and discussed in detail in this article; (■) a thicker AAEM (153 ± 4 μm fully hydrated thickness) that has been detailed in ref 17; (▲) a thinner AAEM (51 ± 2 μm fully hydrated thickness) that has been detailed in ref 13. The filled symbols represent the V_{cell} vs i plots and the open symbols represent the P_{cell} vs i plots.

Previous values of P and Φ for Nafion-117 are reported to be (18 ± 1) × 10^{-7} cm^2 s^{-1} and 1.51 × 10^4 S cm^{-3} s (no indication of errors), respectively;[16,28] however, caution is required when comparing the physical properties of Nafion-115 and Nafion 117 (149 ± 9 and 203 ± 2 μm fully hydrated thicknesses, respectively)[21] as there is growing evidence that physical properties such as equivalent weight (reciprocal to ion-exchange capacity), conductivities, and activation energies for proton conduction are a function of Nafion membrane thickness.[21] A measure of the gravimetric methanol uptakes (Table 1, MU measured using the same method as water uptakes but where the dehydrated membranes were immersed in pure methanol to measure the mass gain) gives a significantly higher value for Nafion-115 than for the AAEM (despite similar water uptakes); this is fully consistent with the permeability measurements above, with Nafion materials exhibiting a higher affinity toward methanol. It is not known at this stage if this lower methanol permeability is an intrinsic property of AAEMs (in relation to Nafion); this is because radiation-grafted PEMs (produced from grafting styrene onto preformed films with subsequent sulfonation to form sulfonic acid functionality) also exhibit reduced methanol permeabilities and so this may be intrinsic to ionomers produced using this synthetic methodology.[29]

The H_2/O_2 fuel cell performance with the AAEM is presented in Figure 5. High catalyst loadings were used so that the same MEA could be used for the hydrogen and methanol fuel cell tests during this study, which is focused on membrane development. The fuel cell containing the AAEM produced for this study exhibited an open circuit voltage (OCV) of 0.99 V and a maximum power density of 94 mW cm^{-2} under the test conditions used. These values can be compared to those obtained with Nafion-115 membranes under almost exactly the same test conditions, the only difference being that Nafion ionomer was painted to

(27) Xue, S.; Yin, G. *Eur. Polym. J.* **2006**, *42*, 776.
(28) Siu, A.; Pivovar, B.; Horsfall, J.; Lovell, K. V.; Holdcroft, S. *J. Polym. Sci., B: Polym. Chem.* **2006**, *44*, 2240.
(29) Scott, K.; Tamma, W. M.; Argyropoulos, P. *J. Membr. Sci.* **2000**, *171*, 119.

similar loadings onto the electrodes using Nafion ionomer dispersed in low aliphatic alcohols (Aldrich, 5% by mass) rather than the alkaline ionomer as described in the Experimental Section above. With this benchmark Nafion-115 MEA, an OCV of 1.04 V and a maximum power density of 290 mW cm^{-2} were obtained. Therefore, this early development AAEM is already producing 33% of the power obtained with Nafion-115 under directly comparable test conditions. This performance is only an order of magnitude below the 900 mW cm^{-2} H_2/O_2 performances that can be obtained with advanced MEAs consisting of catalyzed electrodes using E-Tek Pt/C catalysts, 80 °C operation, and gas supply pressures of 0.4 MPa.[30] This clearly demonstrates the promise of this class of AAEM when applied to fuel cells, especially when the commercial electrode architectures used in this study are evidently not optimized for such application.

The following question needs to be addressed: What is limiting the performance of the AAEM−MEA? The in situ area resistances, measured during fuel cell testing with the AAEM using standard impedance spectroscopy measurements,[31] were 0.9 Ω cm^2 at current densities below 100 mA cm^{-2}, dropping rapidly to 0.6 Ω cm^2 at this point (the onset of this drop is co-incident with the inflection in the V_{cell} vs i plot at this current density). Values in the range 0.6−0.7 Ω cm^2 were obtained with the Nafion-115 benchmark MEA. Therefore, the in situ membrane resistance cannot account for the large loss of performance at low current densities for the AAEM tests. As discussed in an earlier communication,[13] the performance with the AAEM−MEAs appears to be primarily dictated by some form of mass transport limitation. Looking at the fuel cell reactions below,

$$\text{anode: } H_2(g) + 2OH^-(\text{membrane}) \rightarrow 2H_2O(l/g) + 2e^- \quad (4)$$

$$\text{cathode: } H_2O(g/l) + {}^1/_2O_2(g) + 2e^- \rightarrow 2OH^-(\text{membrane}) \quad (5)$$

$$\text{overall: } H_2(g) + {}^1/_2O_2(g) \rightarrow H_2O(l/g) \quad (6)$$

it can be seen that water is a stoichiometric reactant at the cathode (required to generate the OH^- anions). An initial working hypothesis, recently developed from the results of fundamental in situ impedance spectroscopy studies,[2] is that the performances of AAEM−MEAs are being hindered by limited back transport of the water generated by the anode to the required reaction sites at the cathode (the water supplied in the cathode gas stream cannot easily access the oxygen reduction reaction (ORR) sites due to the PTFE binder used in the manufacture of these commercially available electrodes). Figure 5 compares the performance curves, under identical test conditions, obtained with the AAEM from this study with a thicker AAEM and a thinner AAEM (all of similar area resistances). It is evident that the thinner the membrane, the better the H_2/O_2 fuel cell performance (54−94−130 mW cm^{-2} going from the thickest to the thinnest AAEM); this represents clear corroborating evidence for the above hypothesis.

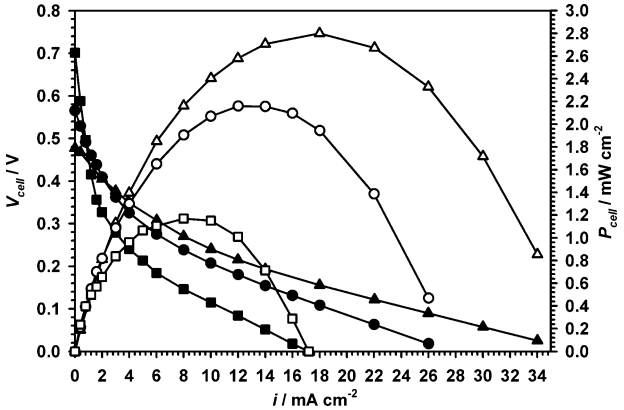

Figure 6. Fuel cell performances (ambient pressures and 50 °C; anode: 4 mg cm^{-2} unsupported PtRu, aqueous methanol (2 mol dm^{-3}) supplied at 10 cm^3 min^{-1}; cathode: 4 mg cm^{-2} unsupported Pt black, O_2 supplied at 2 dm^3 min^{-1}, and RH = 100%) with the following: (●) the ETFE−AAEM (78 ± 3 μm fully hydrated thickness) synthesized and discussed in detail in this article; (■) a thicker AAEM (153 ± 4 μm fully hydrated thickness) that has been detailed in ref 17; (▲) a thinner AAEM (51 ± 2 μm fully hydrated thickness) that has been detailed in ref 13. The filled symbols represent the V_{cell} vs i plots and the open symbols represent the P_{cell} vs i plots.

Figure 6 shows the DMFC performances with the same three AAEMs of different thicknesses. It is immediately evident that the power densities produced are considerably poorer, despite the similar Φ values presented in Table 1, than those obtainable with Nafion-115 MEAs (100−200 mW cm^{-2} power densities are achievable for state-of-the-art Nafion-based DMFCS[32]). Testing the Nafion-115 MEA benchmark described above produced an OCV of 0.66 V and a peak power density of 31 mW cm^{-2}. Again the unoptimized electrode architectures for alkaline MEAs and water mass transport through the AAEMs are the prime suspects leading to poor performance; if methanol permeability or AAEM conductivity were the primary dictators of DMFC performance, then it would be expected that the MEA with the AAEM produced in this study would give a similar performance to a comparable Nafion−MEA, as the values of Φ are similar. The OCVs increased 0.48−0.57−0.70 V on increasing membrane thickness as was expected; thinner membranes of similar chemistry are expected to allow more methanol to cross over than thicker membranes. However, despite the reduced OCVs, the power performances were superior with the thinner membranes (peak powers increasing from 1.2−2.2−2.8 mW cm^{-2} on decreasing membrane thickness); this again is characteristic of the water back-transport hypothesis presented above, with restricted water transport to the cathode contributing to the lower performances.

It is difficult to compare directly the peak powers reported above to literature values, as previous alkaline membrane DMFC studies have used aqueous methanol supplies that contain 1−4 mol dm^{-3} KOH. This was due to a lack of alkaline interface ionomer in the MEAs; the KOH is required to facilitate the transport of the OH^- ions to the anode

(30) Hui, C. L.; Li, X. G.; Hsing, I.-M. *Electrochim. Acta* **2005**, *51*, 711.
(31) Freire, T. J. P.; Gonzalez, E. R. *J. Electroanal. Chem.* **2001**, *503*, 57.
(32) Dillon, R.; Srinivasan, S.; Aricò, A. S.; Antonucci, V. *J. Power Sources* **2004**, *127*, 112.

catalyst reaction sites for reaction with the methanol (6 OH^- ions are required to oxidize 1 CH_3OH molecule). Scott and co-worker have obtained power densities up to 18 mW cm^{-2} at 60 °C using a European commercial AAEM (Morgane-ADP, Solvay S.A., Belgium) with platinized Ti-mesh electrodes (optimized for CO_2 rejection at the methanol anodes) and aqueous methanol supply (2 mol dm^{-3}, supplied at 60 cm^3 min^{-1}) containing KOH (1 mol dm^{-3}).[33] Countanceau et al. obtained 18 mW cm^{-2} at 20 °C using the same AAEM but with aqueous methanol (2 mol dm^{-3}) containing a significantly higher KOH content (4 mol dm^{-3});[34] but <0.5 mW cm^{-2} was achieved when the KOH was removed from the aqueous methanol supply. Ogumi and co-workers achieved 6 mW cm^{-2} at 50 °C with a Japanese commercial AAEM (AHA, Tokuyama, Japan) supplied with aqueous methanol (1 mol dm^{-3} supplied at 50 cm^3 min^{-1}) again with added KOH (1 mol dm^{-3}) and also with a poly(4-vinylpyridine) interface ionomer on the electrodes.[35] These values are all higher than those presented in Figure 6. However, adding KOH into the methanol supply is not desirable for two principal reasons: (1) The KOH constitutes a further chemical component reducing the energy density of the fuel and making this fuel supply highly caustic. (2) The presence of K^+ (or any other M^{n+} cations) in the system will lead to the formation of precipitates of carbonate/bicarbonate on reaction of the OH^- with CO_2 (present either as a product of methanol electro-oxidation or as a natural component of air).

A previously reported medium-term 230 h test has, however, demonstrated that in the absence of any M^{n+} cations and with the use of a solid anion-exchange membrane, and where the counterions are actually the polymer bound $-N^+(CH_3)_3$ sites, performance losses due to carbonation are minimized.[17] Therefore, the emphasis in this study, and all future studies of alkaline membrane direct alcohol fuel cells, must concentrate on metal-cation-free operation.

In summary, the type of AAEM evaluated in this study has, for the first time, the right mix of chemical and physical properties to allow successful application in solid-state M^{n+}-free alkaline fuel cells with power performances at levels that are considered promising. The restricted fuel cell performances stem primarily from the unoptimized electrode architectures used, with impeded mass transport of water to the cathode and methanol to the anode in the methanol case. This confirms the already highlighted[2] requirement for the development of electrode configurations that are specifically targeted for application in alkaline membrane fuel cells. Once suitable electrode architectures have been identified (including those containing non-Pt-metal catalysts), work can then commence on optimization of the fuel cell operating conditions with the ultimate aim of construction of cheap and powerful Pt-free low-temperature fuel cells. It is also clear that the development of high-temperature AAEMs (thermally stable >60 °C) is a further research priority; such an advance would lead to vastly improved membrane conductivities and electrokinetic performances.

Acknowledgment. The authors thank the Engineering and Physical Sciences Research Council of the U.K. for funding (Grant GR\S60709\01) and Keith Lovell (Cranfield University) for γ-ray irradiations.

Supporting Information Available: Delayed contact $^{13}C\{^1H\}$ CP-MAS solid-state NMR spectra of the alkaline anion-exchange membrane. The Raman spectra and thermogravimetric traces of the alkaline anion-exchange membrane, starting materials, intermediate membranes, and related polymers. This material is available free of charge via the Internet at http://pubs.acs.org.

CM062407U

(33) Yu, E. H.; Scott, K. *J. Appl. Electrochem.* **2005**, *35*, 91.
(34) Coutanceau, C.; Lamy, C.; Léger, J.-M.; Demarconnay, L. *J. Power Sources* **2006**, *156*, 14.
(35) Matsuoka, K.; Iriyama, Y.; Abe, T.; Matsuoka, M.; Ogumi, Z. *J. Power Sources* **2005**, *150*, 27.